ChemComm

COMMUNICATION

View Article Online
View Journal | View Issue

Cite this: *Chem. Commun.*, 2024, **60**, 3401

Received 3rd November 2023,
Accepted 19th February 2024

DOI: 10.1039/d3cc05414d

rsc.li/chemcomm

Columnar liquid crystals based on antiaromatic expanded porphyrins†

Duong D. Nguyen,[a] Jorge Labella,*[b] Juan Laforga-Martín,[b] César L. Folcia,[c] Josu Ortega,[c] Tomás Torres,*[bde] Teresa Sierra*[f] and Jonathan L. Sessler*[a]

Three naphthorosarins, antiaromatic expanded porphyrins bearing different *meso* substituents (NRos 1–3), designed to self-assemble into columnar liquid crystalline (LC) structures, were synthesized and characterized using polarized optical microscopy (POM), differential scanning calorimetry (DSC), X-ray diffraction (XRD), as well as supporting computational calculations. The substituents were found to play a crucial role in modulating the LC behaviour.

Supramolecular columnar liquid crystals (LCs) based on π-conjugated organic molecules are promising candidates for the large-scale fabrication of advanced electronic devices.[1] The efficient π–π overlapping in these materials results in intriguing charge-carrier transport properties, where the electrical pathway can be tailored by orienting the assembly using electrical or magnetic fields.[2] In this context, porphyrins (Ps) and phthalocyanines (Pcs) have been widely investigated as building blocks since they provide high-added value technological properties, such as strong absorption in the vis-to-NIR spectral range, modulable band-gaps and excellent processability, just to name a few.[3] Ps and Pcs are based on four-membered pyrrolic skeletons (Fig. 1). However, unique features emerge when the number of pyrrolic units is reduced or increased, leading to the so-called contracted or expanded porphyrinoids, respectively.[4,5]

Expanded porphyrinoids present a wide range of exotic optoelectronic properties (*e.g.*, switchable aromaticity, multistate redox activity, NIR absorption, *etc.*) that are not recapitulated in other organic molecules. As such, they hold great promise for the design and preparation of novel functional materials.[6] To date, contracted porphyrinoids (Fig. 1) have been extensively used for the fabrication of columnar LCs with exciting applications.[7] In contrast, and in spite of their promise, the liquid crystalline expanded derivatives remain almost unexplored. The most recent example dates back to 2007 when our group reported the formation of columnar LCs using cyclo[8]pyrrole (aromatic) co-assembled with electron-deficient additives, which were necessary to direct the columnar assembly through donor–acceptor interactions.[8] The limited development of expanded porphyrin LCs is mainly ascribed to the fact that (i) their synthesis and functionalization are challenging, and that (ii) they often comprise non-planar and flexible π-electron peripheries, which hinders efficient π–π stacking.

β,β′-Phenylene-bridged hexaphyrins[1.0.1.0.1.0], referred to as naphthorosarins (**NRos**; Fig. 1), are a particular class of expanded porphyrinoids characterized by a 24 π-electron conjugated electronic circuit in the ground state, which renders them formally antiaromatic.[9] In contrast to other antiaromatic porphyrinoids, they adopt a planar geometry which imposed by the peripheral annulated benzene rings. Consequently, **NRos** allow for very efficient π–π donor–acceptor interactions both in the solid-state and in organic media. Moreover, they may be

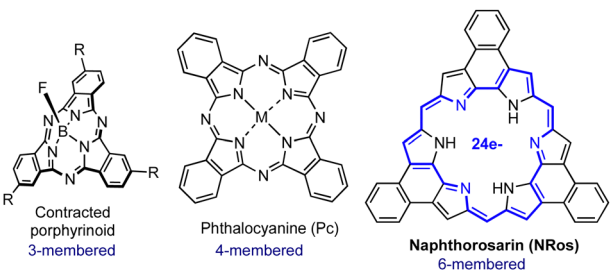

Fig. 1 Molecular structures of 3-, 4- and 6-membered porphyrinoids.

[a] *Department of Chemistry, The University of Texas at Austin, 105 E 24th Street, A5300, Austin, TX, 78712, USA. E-mail: sessler@cm.utexas.edu*
[b] *Department of Organic Chemistry, Universidad Autónoma de Madrid, Campus de Cantoblanco, C/Francisco Tomás y Valiente 7, Madrid 28049, Spain. E-mail: jorge.labella@uam.es, tomas.torres@uam.es*
[c] *Department of Physics, Faculty of Science and Technology, UPV/EHU, Bilbao, Spain*
[d] *Institute for Advanced Research in Chemical Sciences (IAdChem), Universidad Autónoma de Madrid, Madrid 28049, Spain*
[e] *IMDEA-Nanociencia, Campus de Cantoblanco, Madrid 28049, Spain*
[f] *Instituto de Nanociencia y Materiales de Aragón (INMA), Departamento de Química Orgánica, Facultad de Ciencias, CSIC-Universidad de Zaragoza, Zaragoza 50009, Spain*

† Electronic supplementary information (ESI) available. See DOI: https://doi.org/10.1039/d3cc05414d

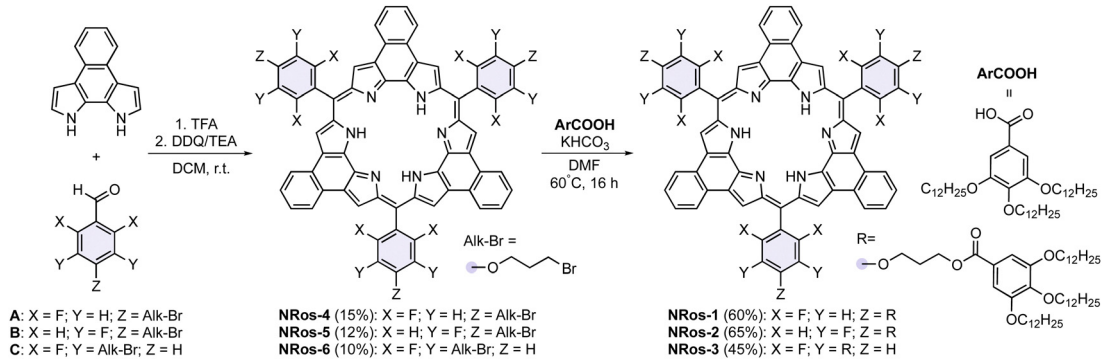

Scheme 1 General synthetic approach for the preparation of **NRos 1–3**.

readily reduced to form 25 π-electron radical anions and 26 π-electron aromatic dianions through proton-coupled electron transfer processes. These inherent features of **NRos** can be fine-tuned by varying the *meso*- and peripheral substituents through use of pre-functionalized naphthobipyrroles or aldehydes as starting materials. We considered it likely that this combination of switchable aromaticity, planarity, and chemical versatility might make **NRos** useful core systems for the development of new liquid crystals (LCs). To test this hypothesis, we synthesized **NRos 1–3** designed to self-assemble into columnar mesophases. As detailed below, these modified **NRos** support the formation of columnar LCs.

The synthetic route to **NRos 1–3** is shown in Scheme 1. These compounds, prepared through a simple two-step process, feature phenyl groups at the *meso* positions. These substituents are further equipped with flexible branched alkyl chains to promote assembly through π–π donor–acceptor and van der Waals interactions. **NRos 1–3** display different substitution patterns (three or six arms at the *meta* or *para* positions) to provide insights into the structure–property relationship. A secondary synthetic objective was to create systems that would allow the role of the aryl fluorine atoms, required for effective macrocyclization, to be assessed. Thus, the first step in our synthesis involved a condensation between naphtho-bipyrrole and aldehydes **A–C**. This provided **NRos 4–6** in 10–15% yield. Subsequently, **NRos 4–6**, bearing alkyl bromide fragments, were subjected to nucleophilic substitution with **ArCOOH**, featuring three dodecyl chains. In this way, **NRos 1–3** were obtained in 60%, 65% and 45% yields, respectively. These compounds were characterized using NMR spectroscopy and high-resolution mass spectrometry.

To determine their LC behaviour, all three compounds were subject to analysis using polarized optical microscopy (POM), differential scanning calorimetry (DSC), and X-ray diffraction (XRD) methods. **NRos-1** exhibited a melting point at 121 °C, as determined by DSC. Upon cooling from the isotropic liquid phase, it displayed a non-fluid birefringent texture. This transition was evident in the DSC thermogram as a broad peak, with a transition temperature of 90 °C and an enthalpy value of 18.2 kJ mol^{-1} (Fig. S7.1, ESI†). The XRD pattern recorded at room temperature revealed two intense reflections in the small angle region, one of them corresponding to a distance of 55.3 Å, with the other reflection (which is somewhat wider than a typical Bragg peak) at 39.1 Å (Fig. S8.1, ESI†). Since they are not related to each other, a columnar structure with rectangular or oblique translation lattice could, in principle, be assumed. On the other hand, several peaks at the medium and wide-angle regions were observed. These latter findings lead us to suggest that **NRos-1** possesses a crystalline structure with a certain degree of disorder, rather than exhibiting LC behaviour. The diffuse halo observed around $2\theta \approx 20^{\circ}$ could reflect disorder within the aliphatic chains.

Under POM examination, **NRos-2** and **NRos-3** became lightly fluid at approximately above 94 °C and 98 °C and fully fluid on heating to 150 °C and 130 °C, respectively. The DSC thermogram of **NRos-2** revealed a very broad thermal transition from *ca.* 150 °C to 280 °C (Fig. S7.2, ESI†). For **NRos-3**, the thermogram didn't show any peak indicative of thermal transition (Fig. S7.3, ESI†). On cooling, neither compound displayed any discernible texture, which could be ascribed to the deep dark color of these samples or to a spontaneous homeotropic alignment.[10] Importantly, mechanical shearing at temperatures around 100 °C allowed non-defined birefringent textures (Fig. S9.1, ESI†) to be observed, which did not change on cooling to room temperature.

Further confirmation of the LC nature of both compounds was achieved through XRD experiments conducted at room temperature. The XRD patterns obtained for **NRos-2** and **NRos-3** (Fig. 2a and b) reveal a diffuse halo at wide angles, a characteristic feature of a LC state. In the small angle region, both compounds exhibit a strong reflection, corresponding to respective distances of 39 Å and 40.3 Å, which are in nice agreement with the calculated diameters of the corresponding fully extended **NRos** cores, excluding the alkyl tails (Fig. 2c). Factors such as the interdigitation of peripheral groups and their flexibility may contribute to lattice parameters smaller than those anticipated for fully extended molecules. Additionally, a weak shoulder at approximately 16 Å is visible for **NRos-2** that is not related to the strong small angle reflection. Variable temperature XRD experiments were carried out to obtain more information on the LC characteristics of both derivatives (see the ESI†). For **NRos-2**, no changes in the XRD pattern were observed upon heating up to 260 °C. In the case of **NRos-3**, the XRD pattern recorded at 125 °C was the typical one of an isotropic liquid state. During the subsequent cooling process, the Bragg reflection characteristic of the mesophase arises at the small angle region showing a clear coexistence of LC order and isotropic liquid disorder (Fig. S8.2, ESI†). This coexistence persists at room temperature and remains visible even after

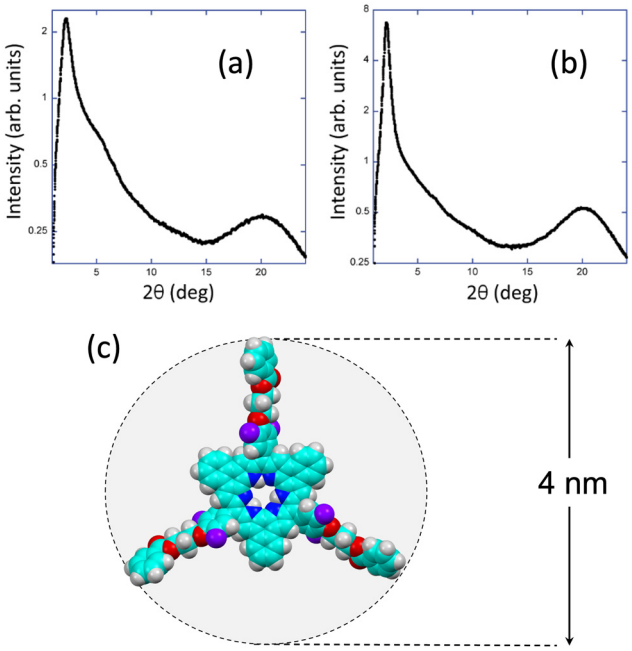

Fig. 2 X-ray diffraction diagram of **NRos-2** (a) and **NRos-3** (b) at room temperature. (c) Theoretical model of the naphthorosarin core.

about 20 h. These findings align with the thermogram, which lacks a clear peak and suggests a gradual transition between the isotropic liquid and the LC phase.

Based on the above results, and considering the disk-like shape of the **NRos** molecules featuring trialkoxybenzoate groups surrounding a planar rigid core, we assume the existence of columnar phases with no long-range stacking order, as deduced from the absence of the 001 reflection maxima at high angles (Fig. S8.2 and S8.3, ESI†).[11] Such a columnar order can be possibly in the form of lamellar for **NRos-3**, and with a two-dimensional rectangular or oblique translation lattice for **NRos-2**. However, we are unable to unambiguously determine the structure of the mesophase, as its two-dimensional structure cannot be confirmed based on the X-ray results.

Theoretical calculations were performed at the GFN2-xTB level to elucidate the origin of the different supramolecular behavior seen for **NRos 1–3**. First, to reduce the computational costs we evaluated the π–π donor–acceptor interactions for the dimers composed of **NRos 1–3** without including the peripheral alkoxy chains. Optimization of **NRos-1** dimers gives rise to structures where the **NRos** molecules do not interact significantly through their π faces (Fig. S6.1a, ESI†). In contrast, both **NRos-2** and **3** are seen to arrange themselves in a π–π face-to-face fashion in their respective self-assembled forms (Fig. S6.1b and c, ESI†). The tendency of **NRos-1** to form stacked dimers in spite of a lack of significant apparent π-facial interactions can be attributed to the perpendicular conformation of the *meso*-aryl groups induced by the *ortho* fluorine atoms, which reduces the conformational flexibility and prevents the accommodation of further molecules on top of each other to form fully columnar structures. By moving (synthetically) the fluorine atoms to the *meta* position, as in **NRos-2**, the *meso*-aryl groups can easily rotate and adopt a more planar structure, thus supporting a π–π stacked structural arrangement. **NRos-3**, despite presenting *ortho*-di-fluorinated *meso*-aryl groups, has six peripheral branches instead of three; these substituents can direct a columnar-type organization by establishing additional van der Waals interactions. Considered in concert, these computational results lead us to conclude that **NRos-2** and **NRos-3** have a higher tendency than **NRos-1** to organize into columns, which is in good agreement with the experimental results.

Next, supramolecular pentamers made up of simplified models of **NRos-2** and **NRos-3** were fully optimized in order to obtain insights into the columnar packing of these molecules (Fig. 3). The **NRos-2** pentamer revealed a highly symmetric, co-axial and helical columnar assembly governed by strong π–π interactions (3.1–3.5 Å). Similar π–π distances have been observed by X-ray diffraction methods in **NRos**-based crystals.[9] When viewed from the top, an inner channel derived from the macrocycle cavity and a 30° rotation between neighboring molecules are seen. In contrast, **NRos-3** pentamers exhibit a much less symmetric organization where the π-skeletons are not as efficiently overlapped, and the peripheral flexible chains are packed in a disordered fashion. Occasionally, these chains establish intermolecular F···π interactions. In comparison to the **NRos-2** pentamer, the π–π interactions between the **NRos-3** antiaromatic cores are less uniform and longer (3.2–3.8 Å), a finding consistent with weaker π–π interactions. Indeed, in the corresponding pentamers, **NRos-2** monomers are essentially planar, whereas in the case of **NRos-3** the monomer displays a saddle-like conformation, presumably to maximize contact of the π-surfaces. These

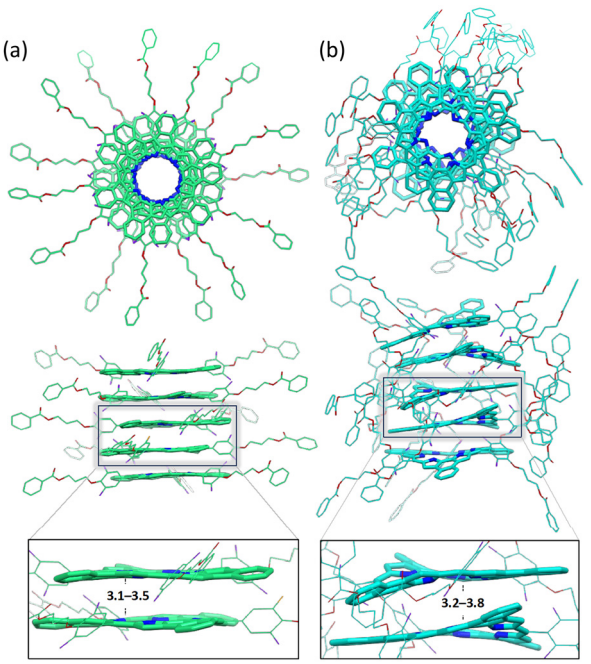

Fig. 3 Top and side views of the supramolecular pentamers of (a) **NRos-2** and (b) **NRos-3** fully optimized at the GFN2-xTB level. Carbons atoms of **NRos-2** and **NRos-3** are represented in green and blue, respectively.

results provide support for the notion that, although the number of peripheral chains is a crucial factor, the position of the fluorine atoms on the *meso*-aryl substituents has a greater impact on the observed packing, at least within this congruent set of **NRos**. Specifically, *meta*-fluorinated aryls allow for planarization and support a face-to-face arrangement.

In summary, we have prepared two liquid-crystalline expanded porphyrins, namely naphthorosarins **NRos-2** and **3**, which exhibit LC behaviour consistent with a columnar organization. Importantly, we have found that the *meso* group determines not only the LC behaviour of this molecule, but also the structure of their corresponding assemblies. The conformational flexibility of these substituents plays a key role in enabling π–π stacking, which appears to be a requirement for achieving the LC behaviour observed by experiment. Theoretical calculations provide support for this suggestion and further revealed that *meta*-substituted *meso*-aryls are suitable groups for producing highly symmetric and co-axial helical columnar assemblies.

Our findings will pave the way for the development of columnar LCs based on expanded porphyrins. Currently efforts are being made to develop LCs based on other expanded derivatives and to explore various technological applications.

The work in Austin was supported by the Robert A. Welch Foundation (F-0018 to J. L. S.). T. T. acknowledges financial support from the Spanish MCIN/AEI/10.13039/501100011033 (PID2020-116490GB-I00, TED2021-131255B-C43), the Comunidad de Madrid and the Spanish State through the Recovery, Transformation and Resilience Plan ["Materiales Disruptivos Bidimensionales (2D)" (MAD2D-CM) (UAM1)-MRR Materiales Avanzados], and the European Union through the Next Generation EU funds. IMDEA Nanociencia acknowledges support from the "Severo Ochoa" Programme for Centres of Excellence in R&D (MINECO, Grant SEV2016-0686). T. T. also acknowledges the Alexander von Humboldt Foundation (Germany) for the A. V. Humboldt – J. C. Mutis Research Award 2023 (Ref. 3.3 - 1231125 - ESP-GSA). J. L. acknowledges MECD, Spain, for a F.P.U. fellowship. We acknowledge the generous allocation of computer time at the Centro de Computación Científica at the Universidad Autónoma de Madrid (CCC-UAM). T. S. acknowledges financial support from PID2021-126132NB-I00 MCIN/AEI/10.13039/501100011033/and by "ERDF A way of making Europe", the Gobierno de Aragón-FSE (E47_23R-research group). C. F. and J. O. acknowledge financial support from the Basque Goverment (Project IT1458-22). C. F. and J. O. acknowledge financial support from the Basque Goverment (Project IT1458-22). The authors would like to acknowledge the Servicios Científico-Técnicos of CEQMA (CSIC-Universidad de Zaragoza) for their support.

Conflicts of interest

There are no conflicts to declare.

Notes and references

1 (*a*) T. Kato, J. Uchida, T. Ichikawa and T. Sakamoto, *Angew. Chem., Int. Ed.*, 2018, **57**, 4355–4371; (*b*) T. Wöhrle, I. Wurzbach, J. Kirres, A. Kostidou, N. Kapernaum, J. Litterscheidt, J. C. Haenle, P. Staffeld, A. Baro, F. Giesselmann and S. Laschat, *Chem. Rev.*, 2016, **116**, 1139–1241; (*c*) S. Sergeyev, W. Pisula and Y. H. Geerts, *Chem. Soc. Rev.*, 2017, **36**, 1902–1929.

2 (*a*) D. Miyajima, F. Araoka, H. Takezoe, J. Kim, K. Kato, M. Takata and T. Aida, *Science*, 2012, **336**, 209–213; (*b*) D. Miyajima, K. Tashiro, F. Araoka, H. Takezoe, J. Kim, K. Kato, M. Takata and T. Aida, *J. Am. Chem. Soc.*, 2009, **131**, 44–45; (*c*) A. S. Tayi, A. Kaeser, M. Matsumoto, T. Aida and S. I. Stupp, *Nat. Chem.*, 2015, **7**, 281–294.

3 (*a*) S. Sengupta, S. Uemura, S. Patwardhan, V. Huber, F. C. Grozema, L. D. A. Siebbeles, U. Baumeister and F. Würthner, *Chem. – Eur. J.*, 2011, **17**, 5300–5310; (*b*) M. Stępień, B. Donnio and J. L. Sessler, *Chem. – Eur. J.*, 2007, **13**, 6853–6863; (*c*) D. Myśliwiec, B. Donnio, P. J. Chmielewski, B. Heinrich and M. Stępień, *J. Am. Chem. Soc.*, 2012, **134**, 4822–4833; (*d*) J. Miao and L. Zhu, *Chem. Mater.*, 2010, **22**, 197–206; (*e*) T. Sakurai, K. Shi, H. Sato, K. Tashiro, A. Osuka, A. Saeki, S. Seki, S. Tagawa, S. Sasaki, H. Masunaga, K. Osaka, M. Tanaka and T. Aida, *J. Am. Chem. Soc.*, 2008, **130**, 13812–13813.

4 (*a*) V. V. Roznyatovskiy, C. Lee and J. L. Sessler, *Chem. Soc. Rev.*, 2013, **42**, 1921–1933; (*b*) S. Saito and A. Osuka, *Angew. Chem., Int. Ed.*, 2011, **50**, 4342–4373; (*c*) T. K. Chandrashekar and S. Venkatraman, *Acc. Chem. Res.*, 2003, **36**, 676–691; (*d*) R. Misra and T. K. Chandrashekar, *Acc. Chem. Res.*, 2008, **41**, 265–279.

5 (*a*) G. Lavarda, J. Labella, M. V. Martínez-Díaz, M. S. Rodríguez-Morgade, A. Osuka and T. Torres, *Chem. Soc. Rev.*, 2022, **51**, 9482–9619; (*b*) J. Labella and T. Torres, *Trends Chem.*, 2023, **5**, 353–366.

6 (*a*) J. L. Sessler and R. A. Miller, *Biochem. Pharmacol.*, 2000, **59**, 733–739; (*b*) J. Kim, J. Oh, A. Osuka and D. Kim, *Chem. Soc. Rev.*, 2022, **51**, 268–292; (*c*) T. Tanaka and A. Osuka, *Chem. Rev.*, 2017, **117**, 2584–2640; (*d*) A. Alka, V. S. Shetti and M. Ravikanth, *Coord. Chem. Rev.*, 2019, **401**, 213063.

7 (*a*) C. Zhang, K. Nakano, M. Nakamura, F. Araoka, K. Tajima and D. Miyajima, *J. Am. Chem. Soc.*, 2020, **142**, 3326–3330; (*b*) M. Lehmann, M. Baumann, M. Lambov and A. Eremin, *Adv. Funct. Mater.*, 2021, **31**, 2104217; J. Guilleme, E. Cavero, T. Sierra, J. Ortega, C. L. Folcia, J. Etxebarria, T. Torres and D. Gonzalez-Rodriguez, *Adv. Mater.*, 2015, **27**, 4280–4284; (*c*) J. Guilleme, J. Arago, E. Orti, E. Cavero, T. Sierra, J. Ortega, C. L. Folcia, J. Etxebarria, D. Gonzalez-Rodriguez and T. Torres, *J. Mater. Chem. C*, 2015, **3**, 985–989.

8 M. Stępień, B. Donnio and J. L. Sessler, *Angew. Chem., Int. Ed.*, 2007, **46**, 1431–1435.

9 (*a*) M. Ishida, S.-J. Kim, C. Preihs, K. Ohkubo, J. M. Lim, B. S. Lee, J. S. Park, V. M. Lynch, V. V. Roznyatovskiy, T. Sarma, P. K. Panda, C.-H. Lee, S. Fukuzumi, D. Kim and J. L. Sessler, *Nat. Chem.*, 2012, **5**, 15; (*b*) D. Firmansyah, S.-J. Hong, R. Dutta, Q. He, J. Bae, H. Jo, H. Kim, K.-M. Ok, V. M. Lynch, H.-R. Byon, J. L. Sessler and C.-H. Lee, *Chem. – Eur. J.*, 2019, **25**, 3525; (*c*) S. Samala, R. Dutta, J. Sessler and C. Lee, *Chem. Commun.*, 2020, **56**, 758; (*d*) G. Kim, R. Dutta, W. Y. Cha, S. J. Hong, J. Oh, D. Firmansyah, H. Jo, K. M. Ok, C. H. Lee and D. Kim, *Chem. – Eur. J.*, 2020, **26**, 16434–16440; (*e*) S. Lee, Y. Wang, R. Dutta, C. H. Lee, J. L. Sessler and D. Kim, *Chem. – Eur. J.*, 2023, **29**, e202301501; (*f*) J. Chen, A. C. Sedgwick, S. Sen, Y. Ren, Q. Sun, C. Chau, J. F. Arambula, T. Sarma, L. Song, J. L. Sessler and C. Liu, *Chem. Sci.*, 2021, **12**, 9916–9921.

10 Y. Kobayashi, A. Muranaka, K. Kato, A. Saeki, T. Tanaka, M. Uchiyama, A. Osuka, T. Aida and T. Sakurai, *Chem. Commun.*, 2021, **57**, 1206–1209.

11 (*a*) M. Peterca, M. R. Imam, P. Leowanawat, B. M. Rosen, D. A. Wilson, C. J. Wilson, X. Zeng, G. Ungar, P. A. Heiney and V. Percec, *J. Am. Chem. Soc.*, 2010, **132**, 11288–11305; (*b*) J. Guilleme, J. Arago, E. Orti, E. Cavero, T. Sierra, J. Ortega, C. L. Folcia, J. Etxebarria, D. Gonzalez-Rodriguez and T. Torres, *J. Mater. Chem. C*, 2015, **3**, 985–989.

